Piezoelectric Transducers for Energy Harvesting: Electromechanical Model, Ambient Motion, and Electrical Loads

Michael L. Isaf, *Graduate Student Member*, *IEEE*, and Gabriel A. Rincón-Mora, *Fellow, IEEE*

***Abstract*— Harvesting ambient kinetic energy can power microsystems that cannot fit batteries large enough to sustain their operational life. Increasing the mechanical-to-electrical conversion efficiency of piezoelectric transducers (PZTs) is critical in this space. A good understanding of how PZTs react to motion and electrical loads is therefore necessary. This is especially true when ambient sources are irregular, which are more prevalent than the often-considered periodic vibrations, and for strongly coupled PZTs. This paper interprets and models PZTs with periodic and irregular sources and energy-harvesting loads. SPICE simulations show and compare the loads' effects on a strongly coupled PZT cantilever's motion.**

***Index Terms*— Piezoelectric Transducer, Electromechanical Model, Continuous/Impulse Source Vibration, Ambient Energy Harvesting, Damped Oscillations, Maximum Power Point**

I. Piezoelectric Harvesters

Ambient energy harvesting is a low maintenance method for powering the ever-growing Internet-of-Things (IoT). Ambient kinetic energy harvesting (EH), specifically, is a good option for powering IoT microsystems since vibrations and motion are prevalent throughout society in mechanical, civil, and biomedical systems [1]–[5].

A common method of motional EH is through piezoelectric transducers (PZTs), as shown in Fig. 1, because they effectively convert energy between the mechanical and electrical domains, have high energy densities, and are readily available off-the-shelf [1], [4]. Motional inputs to the PZT, however, can come in different forms depending on the application. Much of the PZT EH state-of-the-art (SoA) focusses on constant sinusoidal vibrations as the PZT's input motion [1], [4], [5]–[12], but few consider the effects of other types of motion on PZTs. [2]–[4] propose impact based PZT energy harvesters but do not discuss the underlying theory as it pertains to PZT motion. Discussion on modeling PZT initial conditions is also scarce in the SoA.

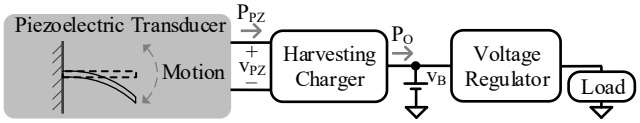

Fig. 1. Piezoelectric harvesting system.

Moreover, electrical loads significantly affect the mechanical motion of strongly coupled (SC) PZTs. Maximum power point (MPP) analysis for weakly coupled PZTs has been studied [10], [11], and [11] discusses resistive load MPPs for SC PZTs, but the effects other EH loads have on motion and MPP is lacking.

This paper presents insightful analysis on the PZT equivalent circuit model in Section II and how various types of motion interact with this model in Section III. Section IV uses SPICE simulations to analyze and compare the effects different EH loads have on SC PZT motion. Section V concludes the paper.

II. Electromechanical Model

Fig. 2 shows a simplified PZT equivalent circuit model with an electrical load to represent the energy transfers occurring during cantilever motion.

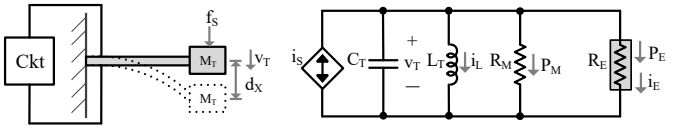

Fig. 2. PZT energy model.

A mass has kinetic energy when in motion with velocity, v_T. Similarly, a capacitor has energy when a voltage develops across it. So, the transducer mass, M_T, in Fig. 2 can be modeled as a capacitor where $C_T \equiv M_T$ [kg], and the mass's velocity, in $\left[\frac{m}{s}\right]$, is equal to the capacitor voltage, v_T, as seen in (1).

$$E_{KE} = 0.5M_T{v_T}^2 \equiv E_C = 0.5C_T{v_T}^2 \quad (1)$$

A mass moves if force is applied to it and a capacitor develops a voltage if current is applied to it. Since v_T represents both voltage and velocity, its time derivative can represent the transducer's acceleration, a_T, and since $C_T \equiv M_T$, the current, i_S, into C_T is analogous to an applied mechanical force, f_S, as seen in (2), in units of $\left[\text{kg}\left(\frac{m}{s^2}\right)\right]$ or [N].

$$i_S = C_T\left(\frac{dv_T}{dt}\right) \equiv M_T a_T = f_S \quad (2)$$

Springs store potential energy when compressed (or bent for a cantilever) a distance, d_X, from rest. Inductors store energy when magnetized by ϕ_L, so an inductor can model a spring with spring constant, K_T, where $\frac{1}{L_T} \equiv K_T\left[\frac{N}{m}\right]$, as (3) shows. i_L represents force applied by the spring. (4) relates d_X to i_L.

$$E_{PE} = 0.5K_T{d_X}^2 \equiv E_L = 0.5\left(\frac{1}{L_T}\right){\phi_L}^2 = 0.5L_T{i_L}^2 \quad (3)$$

$$d_X \equiv \phi_L = i_L L_T \quad (4)$$

Frictional sources, such as air resistance, burn energy and dampen mechanical motion in the same way resistors burn energy in electrical systems. Mechanical dampers, D_M, apply a force in response to motion, so $\frac{1}{R_M} \equiv D_M\left[\frac{kg}{s}\right]$, as seen in (5).

$$D_M = \frac{f_S}{v_T} \equiv G_M = \frac{1}{R_M} = \frac{i_M}{v_T} \quad (5)$$

R_E models a resistive electrical load connected to the PZT. When the PZT oscillates at its resonance frequency, C_T and L_T self-supply, negating their effects on the circuit, so the beam's motion is dominated by R_M's and R_E's equivalent resistance, R_{EQ}, as (6) shows:

$$v_T = i_S R_{EQ} = i_S(R_M||R_E) \quad (6)$$

(7) shows that the losses due to mechanical damping are equal to the power dissipated by R_M. (8) shows that the losses due to the electrical load are equal to the power dissipated by R_E.

$$P_M \equiv G_M {v_T}^2 = \frac{{v_T}^2}{R_M} \tag{7}$$

$$P_E \equiv G_E {v_T}^2 = \frac{{v_T}^2}{R_E} \tag{8}$$

Fig. 3 shows a full PZT mechanical-electrical model. The left side represents the mechanical domain discussed above. The right side represents the electrical domain where C_{PZ} models the PZT's ability to store electrical energy and R_{PZ} models leakage. A Norton equivalent circuit is preferred as R_{PZ} is generally large. The transformer models the energy transfer between the mechanical and electrical domains. k_T is the translation coefficient, representing conversion between force/velocity and current/voltage, and k_C is the coupling coefficient, representing the fraction of energy captured and converted between domains [8], [14].

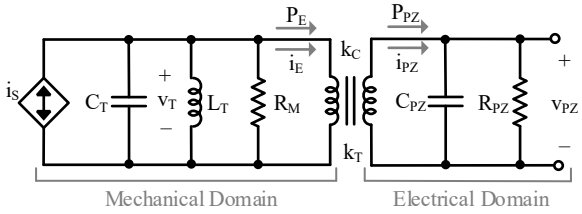

Fig. 3. Full PZT mechanical-electrical model.

III. Ambient Motion

To effectively harvest energy from PZTs, it is important to understand how they behave with different types of input motion. Note that this section analyzes the motion of an unloaded PZT, so R_E is open circuit.

A. Vibrations

Vibrations are perhaps the most researched input to PZTs and can be described as constant periodic oscillations [5]–[11], [14], [15]. Vibrations can be approximated as sinusoids as seen by f_S in Fig. 4. Considering Section II's discussion, a cantilever can be thought of as a resonant filter which suppresses all but the beam's resonant frequency. This is because when the applied vibration period, t_S, is equal to the transducer's resonant period, t_T, periodic oscillations feed the LC tank until C_T and L_T exchange their energy without the help of i_S, therefore, self-supplying. The vibrational energy is then burned by R_M, resulting in sustained oscillations as seen by v_T and d_X in Fig. 4. At frequencies not near resonance, the energy will either be spent predominately on moving the spring, L_T, or the mass, C_T.

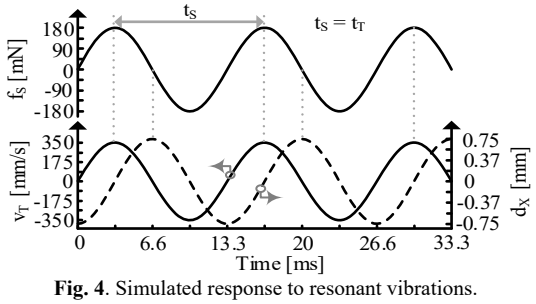

Fig. 4. Simulated response to resonant vibrations.

B. Pulsations

Pulsations are large magnitude motional inputs which occur over a very short time and can be idealized as a Dirac delta function, as seen by f_S in Fig. 5. Pulses or impacts are common in society, from feet hitting the ground to a hammer strike or heartbeat. [2]–[4] take advantage of pulsations by proposing impact harvesters but few have discussed their implications on the PZT model.

An impulse in time is a constant in frequency, so it contains all frequencies. When an input containing all frequencies is applied to a resonant filter, only the resonant frequency remains. So, when a pulsed force acts on the beam, it excites the beam into vibrating at its resonant frequency. The beam's vibration, however, is damped by R_M, so its oscillation will eventually decay to 0, as seen in Fig. 5. The time it takes for the beam's oscillation to reach 5% of its max is the damping time, t_D. Whether or not the oscillation actually decays to 0, though, depends on the source's pulse period, t_S.

Slow Pulsations: Slow pulsations occur when $t_S > t_D$, like Fig. 5 shows. In these cases, the beam's motion can be described as periodic damped resonance as the vibrations will decay to 0 before the next pulse occurs.

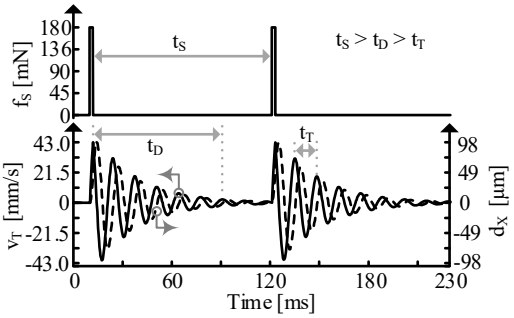

Fig. 5. Simulated response to slow pulsations.

Fast Pulsations: If $t_S < t_D$, fast pulsations occur. In these cases, the beam's motion never completely dies because the impacts supply it with energy packets, counteracting some of the damping that's occurred since the last pulse, as shown in Fig. 6.

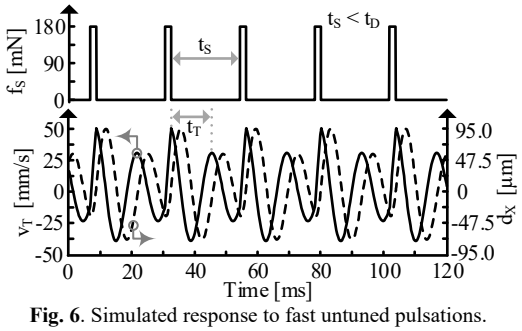

Fig. 6. Simulated response to fast untuned pulsations.

Fig. 7 shows that fast pulses supply energy to the beam most effectively when tuned to one of t_T's harmonics. The most energy is supplied when $t_S = t_T$.

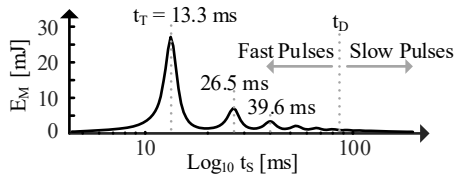

Fig. 7. Mechanical energy across applied pulse period.

C. Initial Conditions

Fig. 8 shows the two initial conditions which can occur for a cantilever [10]. Initial velocity, $v_{T(I)}$, implies that the beam begins its motion with kinetic energy (KE), which can occur by flicking the beam. Initial displacement, $d_{X(I)}$, implies that the beam begins its motion with potential energy (PE).

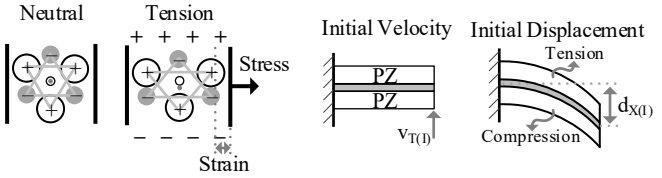

Fig. 8. Cantilevers when flicked and pressed with force.

Rather than using i_S, the beam mass's $v_{T(I)}$ can be modeled as an initial voltage across C_T, and is demonstrated in Fig. 9. Likewise, $d_{X(I)}$ in a spring applies an initial reacting force, so it can be modeled with an initial current, $i_{L(I)}$, in L_T, as modeled in Fig. 10. In both cases, the beam's motion is non-periodic damped resonance since the initial energy supplies the LC tank which then exchanges energy at t_T with continuous loss to R_M.

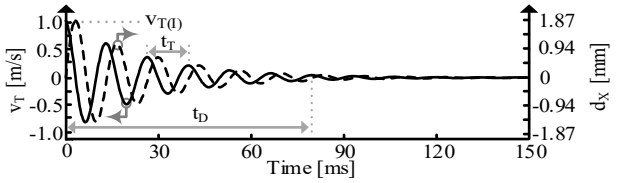

Fig. 9. Simulated response to flicked cantilever.

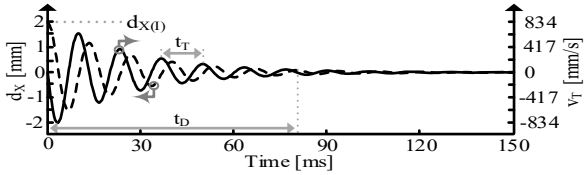

Fig. 10. Simulated response to pressed cantilever.

IV. Electrical Loads

A. Damping

When R_E is applied to a SC PZT with assumed $k_C = 1$ and oscillating at t_T, R_E's magnitude affects the beam's motion. When $R_E \gg R_M$, $R_{EQ} = R_M||R_E \approx R_M$. In this case, R_E is negligible so it's underdamping the system and mechanical damping dominates. This is in line with (4) since $R_E \gg R_M \equiv D_E \ll D_M$. Since Req reaches a max, v_T's peak also maximizes.

R_E's goal, though, is to extract power from the PZT by stealing current/force. While R_E isn't reducing the beam's motion when underdamped (UD), it's also not burning much power. When $R_E \ll R_M$, $R_{EQ} \approx R_E$, so all force from the beam's motion is burned by R_E, but v_T's peak is minimized, reducing motion and available power. This is the overdamped (OD) case.

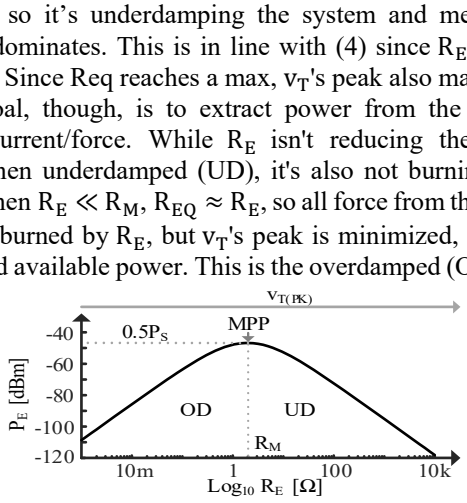

Fig. 11. Electrical power across resistive loads.

The sweet spot for vibration inputs occur when $R_E = R_M$, or $v_T = 0.5v_{T(MAX)}$, because motional loses are balanced with P_E gains, as seen in Fig. 11. Half the source power, P_S, is delivered to R_E when $R_E = R_M$, which is the MPP. Note that this and the following MPPs are for P_E. Ultimately, P_O's MPP is most important when harvesting energy, but that depends on k_C.

B. Electrical Loads

The OD's, UD's, and MPP's effects on motion for a SC PZT are considered for three types of EH loads.

Resistive: Fig. 12 shows the effects a purely resistive load can have on the motion of a beam vibrating at t_T. When UD, R_E has little effect on the beam's motion, so it oscillates as it would in the unloaded case seen in Fig. 4. At the MPP, $R_E = R_M$, so the combined load doubles the mechanical damping resulting in a peak v_T that is half of the uloaded case. If R_E continues to decrease after the MPP, damping will increase until R_E effectively shorts the circuit, so all force from i_S is lost to R_E and no oscillations or motion occur.

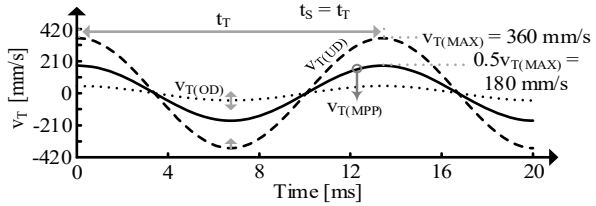

Fig. 12. Simulated response to vibrations with resistive loads.

Synchronized Discharges: Synchronized discharges (SD) occur in switched inductor energy harvesters, which are commonly used in the SoA [6], [8]–[13]. These systems extract packets of PE stored within the spring/inductor when d_X peaks [10]. The damping cases depend on the size of the PE packets extracted relative to the total PE that was present, $PE_{R(E)}$.

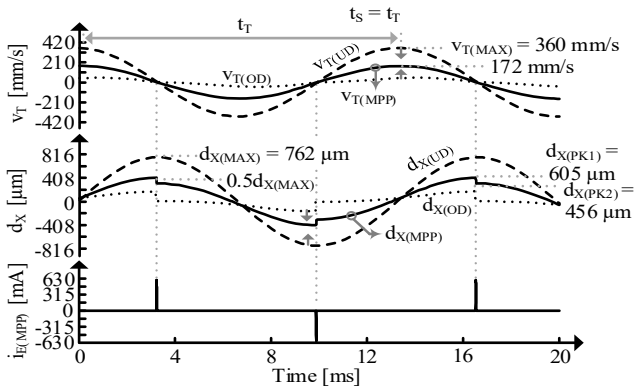

Fig. 13. Simulated responses to vibrations with synced discharges.

The UD extreme occurs when the $PE_{R(E)}$ is very small, so essentially no PE is taken and motion, again, looks the same as in Fig 4. When $PE_{R(E)}$ is too big, the beam's oscillation strength reduces, resulting in motional losses and less available power. This is the OD case. Since PE is extracted when d_X peaks, small oscillations exist even at the OD extreme, so motion can't be completely killed with SD.

When $PE_{R(E)} \approx 0.5$, or $d_{X(PK2)} \approx \frac{d_{X(PK1)}}{\sqrt{2}}$, motional losses are balanced with P_E gains, so the MPP is achieved. Here, SD loads burns approximately the energy stored across a half cycle that resistive loads would have burned during the half cycle. So,

the SD MPP also occurs when $PE_{R(E)}$ reduces v_T to about $0.5v_{T(MAX)}$, as seen in Fig. 13.

Rectified: Many SoA PZT energy harvesters utilize rectifiers [1], [7], [10], [13]. Rectified loads harvests energy from PZTs by channeling a portion of the KE, v_T, at a certain i_L, i_{REC}, to the output, as seen in Fig. 14 [10]. The higher i_{REC}, the more energy that can be harvested with v_T, but more v_T is required to energize L_T to i_{REC}, so less v_T is available for harvesting.

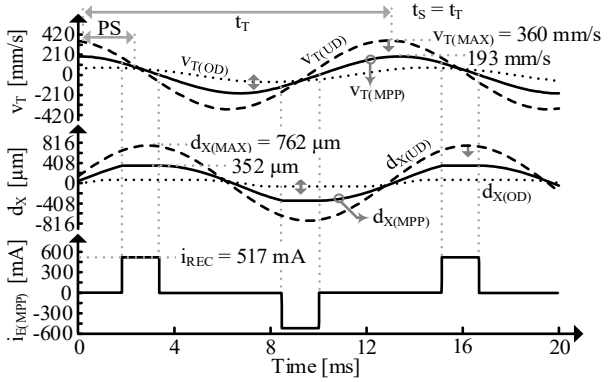

Fig. 14. Simulated response to vibrations with rectified load.

The damping cases depend on i_{REC}. When UD, i_{REC} is so high that i_L never reaches it, so C_T and L_T exchange energy freely, maximizing motion as seen in Fig. 4. When i_{REC} is small, L_T doesn't need much energizing and a lot of v_T is channeled to the load, but the strength at which v_T is harvested is low. Plus, with L_T capped at a low i_L, the LC tank is destroyed and motional loses increase, so the system is OD. i_S receiving energy as i_{REC} drops manifests as a phase shift, PS.

The MPP occurs when i_{REC} gains are balanced with the tradeoff between P_E gains and motional losses associated with capturing more v_T. The rectifier's MPP is not at $0.5v_{T(MAX)}$, unlike for SD and resistive loads.

Comparison: Fig. 15 compares the energy captured by each type of load across v_T. $1 - PE_{R(E)}$ is the relative PE kept in L_T.

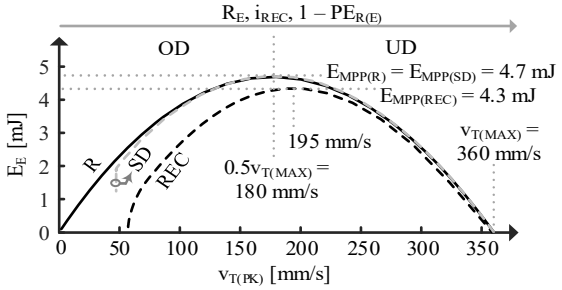

Fig. 15. MPP comparison between electrical loads.

SD and R loads are the most effective options when designing harvesters for SC PZTs since E_E is maximized. $E_{MPP(REC)}$ is lower because the energy required to energize L_T to i_{REC} is never accessible by the harvester. Note that $E_{MPP(REC)}$ occurs at a higher v_T. Note also, that all of the loads converge to a similar UD condition, but respond differently in the OD cases, as was explained above.

V. Conclusions

This paper presented an insightful analysis of the PZT electromechanical model by using a basic understanding of energy transfers and elementary equations. This model was then used to describe and simulate a cantilever style PZT's unloaded response to common motional inputs. Fast pulses always avail more energy than slow pulses but are most effective when tuned to a PZT harmonic. An initial i_L in L_T models initially bent PZTs while an initial v_T across C_T models initially moving PZTs. SPICE simulations showed that resistive and SD loads can draw the most energy from SC PZTs. While all loads respond the same when UD, SD loads have a motional loss limit while rectifiers have the largest motional losses when OD.

References

[1] C. Covaci and A. Gontean, "Piezoelectric Energy Harvesting Solutions: A Review," *Sensors*, vol. 20, no. 12, p. 3512, Jun. 2020.

[2] S. Ju and C. -. Ji, "Indirect impact based piezoelectric energy harvester for low frequency vibration," in *IEEE 2015 Transducers - 2015 18th International Conference on Solid-State Sensors, Actuators and Microsystems*, pp. 1913-1916.

[3] M. Deterre, E. Lefeuvre, Y. Zhu, M. Woytasik, B. Boutaud and R. D. Molin, "Micro Blood Pressure Energy Harvester for Intracardiac Pacemaker," in *IEEE Journal of Microelectromechanical Systems*, vol. 23, no. 3, pp. 651-660, June 2014.

[4] H. Li, C. Tian, and Z. D. Deng, "Energy harvesting from low frequency applications using piezoelectric materials," *Applied Physics Reviews*, vol. 1, no. 4, p. 041301, Nov. 2014.

[5] H. -C. Song *et al*., "Ultra-Low Resonant Piezoelectric MEMS Energy Harvester With High Power Density," in *IEEE Journal of Microelectromechanical Systems*, vol. 26, no. 6, pp. 1226-1234, Dec. 2017.

[6] M. Edla, Y. Y. Lim, D. Mikio and R. V. Padilla, "A Single-Stage Rectifier-Less Boost Converter Circuit for Piezoelectric Energy Harvesting Systems," in *IEEE Transactions on Energy Conversion*, vol. 37, no. 1, pp. 505-514, March 2022.

[7] T. Oh, S. K. Islam, G. To and M. Mahfouz, "Powering wearable sensors with a low-power CMOS piezoelectric energy harvesting circuit," in *2017 IEEE International Symposium on Medical Measurements and Applications (MeMeA)*, 2017, pp. 308-313.

[8] S. Yang and G. A. Rincón-Mora, "Energy-Harvesting Piezoelectric-Powered CMOS Series Switched-Inductor Bridge," in *IEEE Transactions on Power Electronics*, vol. 34, no. 7, pp. 6489-6497, July 2019.

[9] S. Yang and G. A. Rincón-Mora, "Efficient Power Transfers in Piezoelectric Energy-Harvesting Switched-Inductor Chargers," in *IEEE Transactions on Circuits and Systems II: Express Briefs*, vol. 68, no. 4, pp. 1248-1252, April 2021.

[10] G.A. Rincón-Mora and S. Yang, "Tiny piezoelectric harvesters: Principles, constraints, and power conversion," in *IEEE Transactions on Circuits and Systems I*, vol. 63, no. 5, pp. 639–649, May 2016.

[11] D. Guyomar, A. Badel, E. Lefeuvre and C. Richard, "Toward energy harvesting using active materials and conversion improvement by nonlinear processing," in *IEEE Transactions on Ultrasonics, Ferroelectrics, and Frequency Control*, vol. 52, no. 4, pp. 584-595, April 2005.

[12] B. Zhao, J. Wang, W. -H. Liao and J. Liang, "A Bidirectional Energy Conversion Circuit Toward Multifunctional Piezoelectric Energy Harvesting and Vibration Excitation Purposes," in *IEEE Transactions on Power Electronics*, vol. 36, no. 11, pp. 12889-12897, Nov. 2021.

[13] S. Roy, A. N. M. W. Azad, S. Baidya and F. Khan, "A Comprehensive Review on Rectifiers, Linear Regulators, and Switched-Mode Power Processing Techniques for Biomedical Sensors and Implants Utilizing in-Body Energy Harvesting and External Power Delivery," in *IEEE Transactions on Power Electronics*, vol. 36, no. 11, pp. 12721-12745, Nov. 2021.

[14] A. Erturk and D. J. Inman, "A distributed parameter electromechanical model for Cantilevered Piezoelectric Energy Harvesters," in *Journal of Vibration and Acoustics*, vol. 130, no. 4, 2008.

[15] N. G. Elvin and A. A. Elvin, "A general equivalent circuit model for piezoelectric generators," *Journal of Intelligent Material Systems and Structures*, vol. 20, no. 1, pp. 3–9, 2008.